A translational mathematical model linking systemic biomarkers to disease recurrence in diabetic macular edema: a proof-of-concept analysis

Tan Aik Kah

Eye Clinic, Normah Medical Specialist Centre, Kuching, Sarawak, Malaysia

Appendix A: Model 1 (Mechanistic Model): Dynamic Model of DME Progression and Anti-VEGF Response

A.1 Conceptual Framework

DME progression is driven by systemic metabolic factors (HbA1c, BP, and glycemic variability) that influence retinal vascular pathophysiology. In order to model this, we derive a dynamic system that captures (1) VEGF production as a function of HbA1c and BP, (2) Edema formation due to VEGF-driven vascular leakage, and (3) anti-VEGF treatment effect as an impulse function.

A.2 Key Variables

We limit the model to HbA1c, BP, and glycemic variability based on their (1) established mechanistic roles in DME pathogenesis, (2) strong evidence for clinical utility, and (3) feasibility for real-world implementation. While other factors (e.g., lipids, renal function) may contribute to DME, they lack consistent, actionable evidence for guiding anti-VEGF interval adjustments. This precedence is demonstrated by the UKPDS Risk Engine and the CHA_2DS_2-VASc score,[1-2] which are widely adopted for cardiovascular disease (CVD) and stroke risk prediction in atrial fibrillation, respectively, because they effectively balance predictive accuracy with clinical usability by relying on a few key variables.

A.3 Mathematical Model

A.3.1 VEGF Dynamics ($\frac{dV(t)}{dt}$)

A.3.1.1 Biological Basis and Supporting Evidence

A.3.1.1.1 Glycated Hemoglobin (HbA1c)

Numerous studies have demonstrated the link between HbA1c control and treatment outcome with anti-VEGF.[3-6] HbA1c serves as a long-term indicator of glycemic control. Elevated HbA1c levels reflect sustained hyperglycemia, a primary driver of diabetic complications, including DME.[7] Chronic hyperglycemia, in turn leads to the non-enzymatic glycation of proteins and lipids, forming Advanced Glycation End-products (AGEs). These AGEs accumulate in various tissues, including the retina, and plays a pivotal role in the pathogenesis of diabetic vascular complications.[8]

The detrimental effects of AGEs are largely mediated through their interaction with specific cell surface receptors, particularly the Receptor for Advanced Glycation End-products (RAGE). RAGE is expressed on various cell types relevant to retinal vasculature, including endothelial cells, pericytes and Müller glial cells. The bind of AGEs to RAGE initiates a cascade of intracellular signaling events; with the Nuclear Factor-kappa B (NFκB) as one of the most critical activated pathways.[9-10]

NFκB is a transcription factor that, upon activation, translocates to the nucleus and promotes the transcription of numerous genes involved in inflammation, oxidative stress, and angiogenesis. Among the genes up-regulated by NFκB activation is the gene encoding VEGF; a potent cytokine that drives angiogenesis and increases vascular permeability, both of which are central to the development and progression of DME. Increased vascular permeability leads to leakage of fluid and plasma components into the retina, resulting in DME.[11]

A.3.1.1.2 Blood Pressure (BP)

Numerous clinical and population studies have confirmed the association between hypertension and DME.[12-18] Shah et al, on the other hand, has shown that diabetic patients with lower BP required less anti-VEGF treatments.[19] While the precise mechanisms are complex, high BP directly impacts the delicate retinal microvasculature primarily by increasing hydrostatic pressure within the capillaries. The retinal vasculature is characterized by the blood-retinal-barrier (BRB), which is maintained by tightly regulated endothelial tight junctions. Elevated hydrostatic pressure, driven by systemic hypertension, exerts mechanical stress on the endothelial cells lining the retinal capillaries, which in turn causes disruption of the endothelial tight junctions, increasing vascular permeability. Furthermore, chronic hypertension can induce remodeling of the retinal arterioles, leading to vessel constriction and potentially exacerbating downstream hydrostatic pressure in capillaries.[20-22]
While hypertension might not directly up-regulate VEGF synthesis to the same extent as hyperglycemia, the increased hydrostatic pressure and compromised BRB create an environment where even basal levels of VEGF can have a more pronounced effect on leakage. Moreover, endothelial dysfunction induced by hypertension can itself stimulate inflammatory processes and contribute to a pro-angiogenic state, indirectly influencing VEGF.[23]

A.3.1.1.3 Glycemic Variability

Beyond average glycemic control (HbA1c), glycemic variability is increasingly recognized as an independent risk factor for DME.[24-27] The primary mechanism by which glycemic variability contributes to vascular damage and VEGF up-regulation is through the generation of oxidative stress.[28] Rapid changes in glucose concentrations overwhelm the cellular antioxidant defense systems. Intermittent hyperglycemia, in particular, lead to transient but significant increases in reactive oxygen species (ROS) production within endothelial cells and other retinal cells.[29] This "glucose oscillation" effect is believed to be more detrimental than sustained high glucose at a constant level.[30-32]

Oxidative stress, in turn, acts as a potent signaling molecule that activates various pro-inflammatory and pro-angiogenic pathways. Similar to the AGE-RAGE pathway, oxidative stress can activate NFκB and other transcription factors that promote the expression of VEGF.[33-35] It can also impair nitric oxide (NO) bioavailability, further contributing to endothelial dysfunction and increased vascular permeability.[36-38] The damage caused by oxidative stress also destabilizes cellular integrity and can trigger inflammatory responses that amplify VEGF signaling.[39,40]

A.3.1.1.4 Summary

HbA1c, BP, and glycemic variability each contribute through distinct yet interconnected biological pathways of the pathology of DME, primarily by promoting VEGF expression and enhancing vascular permeability. Understanding these fundamental mechanisms provides the biological rationale for integrating these systemic risk factors into a comprehensive model for optimizing anti-VEGF injection intervals.

A.3.1.2 Equation (1)

The rate of change in VEGF concentration is modeled as:

$$\frac{dV(t)}{dt} = P_{sys}(H(t), B(t), G(t)) - \delta_V V(t) - R_{anti}(V(t), I(t))$$

where:

- P_{sys} represents the **systemic driver-induced VEGF production rate**, a function of HbA1c (H), blood pressure (B)**,** and glycemic variability (G). This term aggregates contributions from: (i) HbA1c-mediated advanced glycation end-product (AGE) signaling (AGE–RAGE–NF-κB pathway); (ii) BP-induced hydrostatic and mechanical stress on the vasculature; and (iii) oxidative stress from glycemic variability, which amplifies VEGF transcription and signaling.

The production term aggregates pathogenic contributions:

$$P_{sys} = \alpha_0 + \alpha_H \cdot \max(0, H(t) - H_0)^n + \alpha_B \cdot \max(0, B(t) - B_0) + \alpha_G \cdot \max(0, G(t) - G_0)$$

- γ_v is the natural decay rate constant of VEGF.
- $R_{anti}(V)$ models the saturable anti-VEGF drug effect, formulated using Michaelis-Menten kinetics ($R_{anti}(V) = \delta_v \cdot I(t) \cdot \frac{V(t)}{K_m + V(t)}$) to reflect the finite binding capacity of VEGF ligands.

Thus:

$$\frac{dV(t)}{dt} = \alpha_0 + \alpha_H \cdot \max(0, H(t) - H_0)^n + \alpha_B \cdot \max(0, B(t) - B_0)$$

$$+\alpha_G \cdot \max(0, G(t) - G_0) - \gamma_v \cdot V(t) - \delta_v \cdot I(t) \cdot \frac{V(t)}{K_m + V(t)}$$

where:

- $V(t)$: VEGF at time t (pg•mL^{-1})
- α_0 : baseline VEGF production rate (pg•mL^{-1}•day^{-1})
- $\alpha_H, \alpha_B, \alpha_G$: Scaling coefficients for pathological VEGF production driven by excess HbA1c, BP, and glycemic variability, respectively (with units pg•mL^{-1}•day^{-1}•%$^{-n}$,
- pg•mL^{-1}•day^{-1}•mmHg^{-1}, pg•mL^{-1}•day^{-1}•%CV^{-1})
- $H(t), B(t), G(t)$: Time-varying HbA1c (%), systolic BP (mmHg), and glycemic variability (%CV)
- H_0, B_0, G_0 : Threshold values for pathogenic onset of each driver
- n : Hill coefficient (modeling AGE–RAGE cooperativity; assumed $n = 2$)
- γ_v : VEGF clearance rate (day^{-1})
- δ_v : Maximum rate of VEGF removal due to anti-VEGF (pg•ml-1day-1)
- $I(t)$: Anti-VEGF treatment indicator, a binary function (1 at injection, 0 otherwise). This is a simplification representing the immediate presence of drug.
- K_m : Michaelis constant (pg•mL^{-1}), represents the VEGF concentration at which the anti-VEGF removal rate is half of its maximum ($\delta_V/2$). It provides a measure of the "affinity" or efficiency of the anti-VEGF effect at lower VEGF concentrations.

A.3.1.3 Interpretation and Plausibility of Equation (1)

The equation models VEGF dynamics as a balance between production and clearance (decay and anti-VEGF effect).

A.3.1.3.1 HbA1c-driven VEGF production

High HbA1c leading to increased VEGF production is well established.[41-43] The concept of HbA1c threshold (H_0) is plausible, as a certain level of HbA1c may be considered normal or insufficient to induce VEGF production. The Hill coefficient for cooperativity ($n = 2$) for AGE-RAGE coorperativity, consistent with receptor-ligand binding kinetics, suggests a non-linear and potentially accelerating response.[44]

A.3.1.3.2 α_0 (baseline VEGF production rate)

In order to ensure biological realism, the model incorporates a basal VEGF production rate. This acknowledges that VEGF is constitutively expressed at low levels even in healthy individuals, playing essential roles in vascular homeostasis and normal retinal function. While pathological stimuli from elevated HbA1c and BP drive an increase in VEGF production, a non-zero baseline is crucial for accurately representing physiological processes. This aligns with observation that vitreous VEGF is detectable even in normoglycemic states, with production rising nonlinearly in response to hyperglycemia.[45]

A.3.1.3.3 Threshold behavior ($\max(0, H(t) - H_0), \max(0, B(t) - B_0), \max(0, G(t) - G_0)$)

This captures the idea that VEGF production only escalates when HbA1c, BP, or glycemic variability exceed critical thresholds (e.g., HbA1c > 7%, systolic BP > 140 mm Hg, glycemic variability > 33%). Biologically, this aligns with (1) HbA1c: AGE-RAGE signaling activates NFκB only when AGEs accumulate beyond a threshold,[11] (2) BP: Starling forces disrupt endothelial tight junctions only above a pressure threshold,[23] and (3) glycemic variability: oxidative stress acts as a potent signaling molecule that activates various pro-inflammatory and pro-angiogenic pathways.[34]

A.3.1.3.4 Linear BP term

The effect of hypertension on VEGF is likely dose-dependent (no saturation observed clinically), therefore a linear term is reasonable.

A.3.1.3.5 Linear Glycemic Variability term

A linear relationship is a reasonable starting point for modeling the effect of glycemic variability. While biological responses can be complex, a simple linear driver provides a direct and interpretable link between glycemic variability and VEGF production. This can be refined later if data suggests a non-linear relationship (e.g., using a threshold or saturating function). For now, a linear term implies that any increase in variability, even from low levels, contributes to VEGF production, which is plausible.

A.3.1.3.6 VEGF decay (γ_v)

VEGF decay follows first-order kinetic process, which is justifiable for a relatively well-mixed compartment like the vitreous humor. Enzymatic degradation and receptor-mediated uptake (if not saturated) are proportional to the amount of available VEGF. Diffusion/bulk flow clearance for small molecules are often approximated as first-order.[46]

A.3.1.3.7 Anti-VEGF effect

The use of a constant parameter (δ_v) representing the maximum rate of VEGF removal due to anti-VEGF therapy, is justified for the purpose of modeling dosing intervals in clinical practice. This approach captures the peak pharmacodynamic effect of anti-VEGF immediately following administration, which is the most clinically relevant period for determining where re-treatment may be necessary. By focusing on the time, it takes for VEGF levels to rise again after being maximally suppressed, the model can predict when therapeutic efficacy begins to wane—informing appropriate dosing intervals. This simplification avoids unnecessary complexity in modeling drug kinetics while still providing a biologically meaningful and clinically actionable representation of anti-VEGF activity over time.

Binary $I(t)$. This modeling approach employs discrete, rather than continuous, anti-VEGF administration to align with real-world clinical protocols and enhance practical utility. The primary objective is direct clinical translation. Utilizing a binary representation for $I(t)$ (indicating presence or absence of drug effect) offers sufficient predictive power for determining optimal injection intervals. This aligns with the clinically pragmatic nature of binary decisions (e.g., "extend" or "do not extend" treatment intervals), facilitating straightforward application in real-world patient management.

The use of a **Michaelis-Menten kinetic** for anti-VEGF effect makes excellent biological and medical sense due to the principle of saturable binding and drug kinetics. At low VEGF concentration ($V(t) \leq K_m$), the removal rate is approximately linear with VEGF concentration. At high VEGF concentration ($V(t) > K_m$), the removal rate approaches a

maximum value (δ_v). This signifies that anti-VEGF drug's binding capacity or neutralizing capacity becomes saturated, and it can only remove VEGF at a maximum rate, regardless of how much more VEGF is present. This is crucial for understanding why very high VEGF levels might not be fully controlled by a fixed dose of anti-VEGF.[47]

A.3.2 Macular Edema Dynamics ($\frac{dC(t)}{dt}$)

A.3.2.1 Biological Basis and Supporting Evidence

Fluid accumulation in the macula disrupts the precise architecture of the photoreceptors, leading to impaired visual acuity. The underlying pathophysiology of DME is multifaceted, involving a complex interplay of vascular abnormalities, inflammatory processes, and metabolic dysregulation, primarily driven by chronic hyperglycemia and associated systemic co-morbidities. The dynamics of DME are rooted in a balance between fluid extravasation from the retinal blood vessels and its subsequent clearance from the macula, modulated by various physiological and therapeutic factors.

A.3.2.1.1 VEGF-Driven Leakage: The Primary Driver of Fluid Extravasation

VEGF is a significant pathological mediator of vascular permeability in DME.[48] In hyperglycemic conditions, retinal cells (pericytes, endothelial cells, Müller cells) become hypoxic or metabolically stressed, leading to an up-regulation of VEGF production.[11] Elevated intraocular VEGF directly increases vascular permeability. VEGF binds to its receptors (VEGFR-2) on endothelial cells, leading to phosphorylation of tight junction proteins (e.g., occludins, claudins, zonula occludens-1), disruption of intercellular junctions, and formation of fenestrations.[49-53] This compromise of the BRB allows plasma components, including fluid and proteins, to leak into the retinal extracellular space, forming edema.

The leakage is not endlessly linear with increasing VEGF concentration. Endothelial cell receptors for VEGF can become saturated at high VEGF levels (Michaelis-Menten kinetics). There is a physiological delay between the increase in VEGF concentration and the onset of measurable fluid extravasation. This lag time (τ) accounts for the cascade of events required for VEGF to induce changes in endothelial cell permeability, including receptor binding, intracellular signaling, and subsequent structural alterations to vessel integrity. This is consistent with clinical observations where treatment effects on fluid resolution are not instantaneous.[54,55]

Anti-VEGF therapy is the cornerstone of DME management. While their primary action is to neutralize VEGF, this neutralization rapidly reduces vascular permeability, which subsequently leads to a more efficient resolution of existing fluid.[56,57]

A.3.2.1.2 Fluid Clearance: Modulated by Systemic Factors and Treatment

The resolution of DME depends on the effective removal of accumulated fluid by the retinal drainage systems. This clearance is a dynamic process influenced by baseline physiological mechanisms, systemic blood pressure, and therapeutic interventions. Baseline passive fluid clearance (active transport systems, diffusion, and bulk flow into the RPE and choroidal circulation) is fundamental for maintaining retinal homeostasis, even under pathological conditions.[58] The role of hypertension in the development and progression of DME was discussed in section A.3.1.1.2

A.3.2.1.3 Glycemic Variability-VEGF Synergy Effect: A Potentiating Factor

The role of glycemic variability was discussed in section A.3.1.1.3. glycemic variability can potentiate the detrimental effects of VEGF on vascular leakage synergistically. This means that even at moderate VEGF levels, high glycemic variability can significantly amplify leakage, driving edema formation.[29-32,59]

A.3.2.1.4 Summary

This comprehensive biological framework underscores that DME is a dynamic process shaped by a complex interplay of VEGF-driven permeability, multifactorial fluid clearance mechanisms, and the exacerbating influence of glycemic variability, providing a robust foundation for the subsequent equation (2).

A.3.2.2 Equation (2): Macular Edema Dynamics

The rate of change in central macular thickness is modeled as:

$$\frac{dC(t)}{dt} = L(V(t), G(t)) - F_{clear}(B(t), I(t)) \cdot C(t)$$

where:

- $L(V, G)$ is the **total leakage function** into the retina, which depends on VEGF and glycemic variability.

- F_{clear} is the **total fluid clearance rate function**, which depends on systemic blood pressure and anti-VEGF treatment.

Leakage Term $L(V, G)$: Retinal leakage is driven by two interconnected pathways:

1. A primary, **saturable pathway** directly activated by VEGF, following Michaelis-Menten kinetics with a time lag τ.

2. A secondary, **VEGF-dependent pathway** that is **modulated by glycemic variability**. This term captures the hypothesis that oxidative stress from high glycemic variability creates a permissive environment that enables additional leakage proportional to the present VEGF level.

   $L(V, G)$ =Saturable VEGF Leakage + glycemic variability -modulated VEGF Leakage

$$= k_v \cdot \frac{V(t-\tau)}{K_m + V(t-\tau)} + \sigma_G \cdot \max(0, G(t) - G_0) \cdot V(t)$$

Clearance Term F_{clear}: Fluid clearance is modeled as a first-order process proportional to the existing thickness $C(t)$. The clearance rate constant is impaired by elevated blood pressure and enhanced by anti-VEGF therapy.

$$F_{clear} = [k_{c0} + \frac{k_{c1}}{1 + \beta \cdot \max(0, B(t) - B_0)} + \delta_c \cdot I(t)] \cdot C(t)$$

Full combined equation:

$$\frac{dC(t)}{dt} = k_v \cdot \frac{V(t-\tau)}{K_m + V(t-\tau)} + \sigma_G \cdot \max(0, G(t) - G_0) \cdot V(t)$$

$$-[k_{c0} + \frac{k_{c1}}{1 + \beta \cdot \max(0, B(t) - B_0)} + \delta_c \cdot I(t)] \cdot C(t)$$

where

- $C(t)$: Central macular thickness at time t (μm)
- $V(t)$: VEGF concentration at time t (pg•mL^{-1})
- τ : Time lag for VEGF effect on vascular permeability (days)
- k_v : Maximal rate of the saturable VEGF leakage pathway (μm•day^{-1})
- K_m : Michaelis constant for the saturable leakage pathway (pg•mL^{-1})
- σ_G : Coefficient for glycemic variability -modulated leakage (μm•day^{-1}•(pg/mL)$^{-1}$•%CV^{-1})
- $G(t)$: glycemic variability at time t (percent coefficient of variation, %CV)
- G_0 : Threshold of glycemic variability for activating the secondary leakage pathway (%CV)
- k_{c0} : Baseline passive clearance rate constant (day^{-1})
- k_{c1} : Amplitude of the pressure-sensitive clearance component (day^{-1})
- β : Coefficient for blood pressure impairment of clearance (mmHg^{-1})
- $B(t)$: Systolic blood pressure at time t (mm Hg)
- B_0 : Blood pressure threshold for impairing clearance (mm Hg)
- δ_c : Anti-VEGF treatment-enhanced clearance rate constant (day^{-1})
- $I(t)$: Anti-VEGF treatment indicator (binary: 1 at injection, 0 otherwise)

A.3.2.3 Interpretation and Plausibility of Equation (2)

Equation (2) captures the temporal evolution of central macular thickness $C(t)$ as influenced by VEGF-mediated leakage, clearance mechanisms modulated by BP and anti-VEGF therapy, and the synergistic interaction between glycemic variability and VEGF.

A.3.2.3.1 Saturable VEGF-Driven Leakage

This term models the leakage of fluid into the retinal tissue driven by VEGF. VEGF-A increases endothelial permeability by altering the integrity of tight junctions in retinal capillaries, promoting protein-rich plasma extravasation into the extracellular space.[60] The use of a Michaelis-Menten-type saturation function reflects the fact that VEGF receptors (VEGF-2 in particular) become saturated at higher VEGF concentrations, beyond which further increases in VEGF do not linearly increase leakage. This concept is supported by studies showing that VEGF-induced permeability exhibits a nonlinear dose-response relationship.[49-53] The **delay term $\boldsymbol{\tau}$** (1-2 days) captures the lag between VEGF elevation and peak leakage, consistent with biological observations in both experimental diabetic retinopathy and VEGF-injection models, where fluid accumulation occurs with a latency after VEGF exposure.[54,55]

A.3.2.3.2 Blood Pressure and Treatment-Dependent Fluid Clearance

$\boldsymbol{k_{c0}}$ models baseline passive reabsorption of interstitial fluid through the retinal pigmented epithelium (RPE) and choroid.

$\frac{\boldsymbol{k_{c1}}}{\mathbf{1}+\boldsymbol{\beta}\cdot\mathbf{max}(\mathbf{0},\boldsymbol{B}(\boldsymbol{t})-\boldsymbol{B_0})}$ represents dynamic clearance that is inversely dependent on the systemic BP. Elevated BP may impair clearance by increasing hydrostatic pressure in the retinal capillaries, thus opposing the transretinal osmotic gradient required for fluid reabsorption. Shah et al have shown that hypertensive patients with DME have more persistent edema and require more frequent anti-VEGF therapy.[19]

$\boldsymbol{\delta_c}\cdot\boldsymbol{I}(\boldsymbol{t})$ accounts for enhanced clearance induced by anti-VEGF therapy. VEGF inhibition restores endothelial integrity and reduced fluid ingress, indirectly improving the function of clearance mechanisms. Anti-VEGF also down-regulates inflammatory

cytokines that may block fluid outflow pathways, supporting its inclusion as a clearance-boosting factor.[61]

The entire expression in multiplied by $\boldsymbol{C(t)}$, consistent with first-order kinetics where greater fluid volume drives faster reabsorption, until a clearance capacity become saturated or impaired.

A.3.2.3.3 Glycemic Variability-VEGF Synergy Effect

This term models the amplifying effect of glycemic variability on VEGF-induced vascular dysfunction. glycemic variability is an independent risk factor for endothelial damage and oxidative stress in DME; it promotes AGEs, mitochondrial dysfunction, and inflammation, all of which sensitize retinal vessels to VEGF-mediated permeability.[24,27]

The multiplicative form of $\max(0, G(t) - G_0) \cdot V(t)$ is biologically justified: while VEGF inherently causes leakage, this effect is potentiated in a pro-inflammatory, pro-oxidative environment driven by glycemic variability. Both *in vitro* and *in vivo* studies, have shown hyperglycemic oscillations to exaggerate VEGF expression and endothelial response to VEGF stimuli.[30-33,59] Therefore, this term models a pathological synergy where glycemic variability primes the retina to respond more aggressively to even modest VEGF levels.

A.4 Phase-Plane Analysis

To move from the formulation of the model to an understanding of its clinical implications, we perform a phase-plane analysis. This examines the long-term behavior (equilibria and stability) of the coupled system of VEGF and macular thickness under different clinical scenarios, revealing the fundamental dynamics that dictate treatment response and recurrence.

A.4.1 Case 1 (Baseline Scenario): Controlled Systemic Parameters; $H(t) = H_0$, $B(t) = B_0$, $G(t) = G_0$, No Treatment ($I(t) = 0$) [Figure A1]

In this baseline scenario, systemic parameters related to the disease progression are kept at their healthy or threshold levels. This means HbA1c (H(t)) is at its baseline (H_0), BP and glycemic variability are at their thresholds (B_0 and G_0). Under these controlled conditions, the production terms for VEGF due to elevated HbA1c, BP, and glycemic variability would be zero. The system's equilibrium points are found by setting the rates of change to zero, yielding the nullclines.

A.4.1.1 VEGF nullcline ($\frac{dV(t)}{dt} = 0$): With $H(t) = H_0$, $B(t) = B_0$, $G(t) = G_0$, and $I(t) = 0$

From equation (1):

$$\frac{dV(t)}{dt} = \alpha_0 + \alpha_H \cdot \max(0, H(t) - H_0)^n + \alpha_B \cdot \max(0, B(t) - B_0)$$

$$+\alpha_G \cdot \max(0, G(t) - G_0) - \gamma_v \cdot V(t) - \delta_v \cdot I(t) \cdot \frac{V(t)}{K_m + V(t)}$$

$$0 = \alpha_0 + \alpha_H \cdot \max(0, H_0 - H_0)^n + \alpha_B \cdot \max(0, B_0 - B_0)$$

$$+\alpha_G \cdot \max(0, G_0 - G_0) - \gamma_v \cdot V(t) - \delta_v \cdot 0 \cdot \frac{V(t)}{K_m + V(t)}$$

$$= \alpha_0 + \alpha_H \cdot 0 + \alpha_B \cdot 0 + \alpha_G \cdot 0 - \gamma_v \cdot V(t) - 0$$

$$= \alpha_0 - \gamma_v \cdot V(t)$$

Thus: $\alpha_0 = \gamma_v \cdot V(t)$

$$V(t) = \frac{\alpha_0}{\gamma_v}$$

$V_{nullcline}$ represents a stable, basal VEGF concentration essential for physiological function, as indicated by the presence of the basal VEGF production rate (α_0). This reflects the physiological necessity of a baseline VEGF concentration for normal vascular function, even in the absence of pathological stimuli.

The nullcline represents an equilibrium where the rate of VEGF production is precisely balanced by its removal rates. This equation shows a complex interplay between basal production (α_0), natural VEGF decay (γ_v). This specific nullcline represents the minimal steady-state VEGF level achievable when HbA1c, BP, and glycemic variability are all at their respective physiological thresholds (H_0, B_0, G_0). Under these ideal conditions, the pathological VEGF production pathways driven by these systemic risk factors are entirely suppressed or inactive. Therefore, VEGF dynamics are governed by intrinsic production and distinct clearance mechanism (linear natural decay).

A.4.1.2 Central Macular Thickness ($\frac{dC(t)}{dt} = 0$): With $\boldsymbol{H(t) = H_0}$, $\boldsymbol{B(t) = B_0}$, $\boldsymbol{G(t) = G_0}$, and $\boldsymbol{I(t) = 0}$

From equation (2):

$$\frac{dC(t)}{dt} = k_v \cdot \frac{V(t-\tau)}{K_m + V(t-\tau)} + \sigma_G \cdot \max(0, G(t) - G_0) \cdot V(t)$$

$$-[k_{c0} + \frac{k_{c1}}{1 + \beta \cdot \max(0, B(t) - B_0)} + \delta_c \cdot I(t)] \cdot C(t)$$

Since the delay τ is small, and the system is in steady state, $V(t-\tau) \approx V(t)$

$$0 = k_v \cdot \frac{V(t)}{K_m + V(t)} + \sigma_G \cdot \max(0, G_0 - G_0) \cdot V(t)$$

$$-[k_{c0} + \frac{k_{c1}}{1 + \beta \cdot \max(0, B_0 - B_0)} + \delta_c \cdot 0] \cdot C(t)$$

$$= k_v \cdot \frac{V(t)}{K_m + V(t)} + \sigma_G \cdot 0 \cdot V(t)$$

$$-[k_{c0} + \frac{k_{c1}}{1 + \beta \cdot 0} + \delta_c \cdot 0] \cdot C(t)$$

$$= k_v \cdot \frac{V(t)}{K_m + V(t)} - [k_{c0} + k_{c1}] \cdot C(t)$$

Thus:

$$[k_{c0} + k_{c1}] \cdot C(t) = k_v \cdot \frac{V(t)}{K_m + V(t)}$$

$$C(t) = \frac{k_v}{k_{c0} + k_{c1}} \cdot \frac{V(t)}{K_m + V(t)}$$

The central macular thickness nullcline, $C_{nullcline}$ indicates that the steady-state central macular thickness. It is directly related to the VEGF concentration at the lagged time point $V(t - \tau)$ in a saturable kinetics, characteristics of a Michaelis-Menten-like behavior. **At low VEGF levels (when $\boldsymbol{V(t) \ll K_m}$**, the equation simplifies to:

$$C_{nullcline} \approx \frac{k_v}{k_{c0} + k_{c1}} \cdot \frac{V(t)}{K_m}$$

In this regime, the steady-state central macular thickness is approximately linearly proportional to the VEGF concentration. **At high VEGF levels (when $\boldsymbol{V(t) \gg K_m}$),** the equation simplifies to:

$$C_{nullcline} \approx \frac{k_v}{k_{c0} + k_{c1}} \cdot \frac{V(t)}{V(t)} = \frac{k_v}{k_{c0} + k_{c1}}$$

In this regime, the central macular thickness approaches a maximum plateau, determined by the maximal leakage rate and the total clearance capacity, regardless of further increases in VEGF.

The steady-state central macular thickness is inversely proportional to the sum of the baseline passive fluid clearance (k_{c0}) and the dynamic fluid clearance (k_{c1}). This means that higher inherent capabilities to remove fluid from the macula (stronger clearance mechanisms) lead to lower equilibrium fluid accumulation. It is also directly proportional to the maximal leakage rate (k_v). A greater inherent tendency for the

retinal blood vessel to leak fluid will result in a proportionally higher equilibrium level of the macular edema.

In essence, $C_{nullcline}$ describes the equilibrium central macular thickness that would be established purely by the dynamic between the inherent (saturable) VEGF-driven fluid leakage and the intrinsic physiological fluid clearance mechanisms, under conditions where systemic risk factors (BP, glycemic variability) are well controlled and no anti-VEGF treatment is applied.

A.4.1.3 Phase Plane Portrait

2.4.1.3.1 Equilibrium point

When $V(t) = \frac{\alpha_0}{\gamma_v}$:

$$\frac{dC(t)}{dt} = k_v \cdot \frac{V(t)}{K_m + V(t)} - [k_{c0} + k_{c1}] \cdot C(t)$$

$$= k_v \cdot \frac{\frac{\alpha_0}{\gamma_v}}{K_m + \frac{\alpha_0}{\gamma_v}} - [k_{c0} + k_{c1}] \cdot C(t)$$

When $\frac{dC(t)}{dt} = 0$:

$$0 = k_v \cdot \frac{\frac{\alpha_0}{\gamma_v}}{K_m + \frac{\alpha_0}{\gamma_v}} - [k_{c0} + k_{c1}] \cdot C(t)$$

$$C(t) = \frac{k_v}{k_{c0} + k_{c1}} \cdot \frac{\frac{\alpha_0}{\gamma_v}}{K_m + \frac{\alpha_0}{\gamma_v}}$$

Thus, the equilibrium point:

$$\left(\frac{\alpha_0}{\gamma_v}, \frac{k_v}{k_{c0} + k_{c1}} \cdot \frac{\frac{\alpha_0}{\gamma_v}}{K_m + \frac{\alpha_0}{\gamma_v}}\right)$$

A.4.1.3.2 Vectors along the $V_{nullcline}$

When $\frac{dC(t)}{dt} > 0$:

$$k_v \cdot \frac{\frac{\alpha_0}{\gamma_v}}{K_m + \frac{\alpha_0}{\gamma_v}} - [k_{c0} + k_{c1}] \cdot C(t) > 0$$

$$C(t) < \frac{k_v}{k_{c0}+k_{c1}} \cdot \frac{\frac{\alpha_0}{\gamma_v}}{K_m+\frac{\alpha_0}{\gamma_v}} \qquad \text{(vectors point upward)}$$

Conversely, when $\frac{dC(t)}{dt} < 0$:

$$C(t) > \frac{k_v}{k_{c0}+k_{c1}} \cdot \frac{\frac{\alpha_0}{\gamma_v}}{K_m+\frac{\alpha_0}{\gamma_v}} \qquad \text{(vectors point downward)}$$

2.4.1.3.3 Vectors along the $C_{nullcline}$

From section A.4.1.1, when $\frac{dV(t)}{dt} = 0$:

$$V(t) = \frac{\alpha_0}{\gamma_v}$$

when $\frac{dV(t)}{dt} > 0$:

$$V(t) < \frac{\alpha_0}{\gamma_v} \qquad \text{(vectors point rightward)}$$

Conversely, when $\frac{dV(t)}{dt} < 0$:

$$V(t) > \frac{\alpha_0}{\gamma_v} \qquad \text{(vectors point leftward)}$$

A.4.1.3.4 Stability of the equilibrium point

From the phase plane portrait, the equilibrium point is a **sink (stable).**

Figure A1: Phase plane analysis of central macular thickness (CMT) dynamics in Case 1.

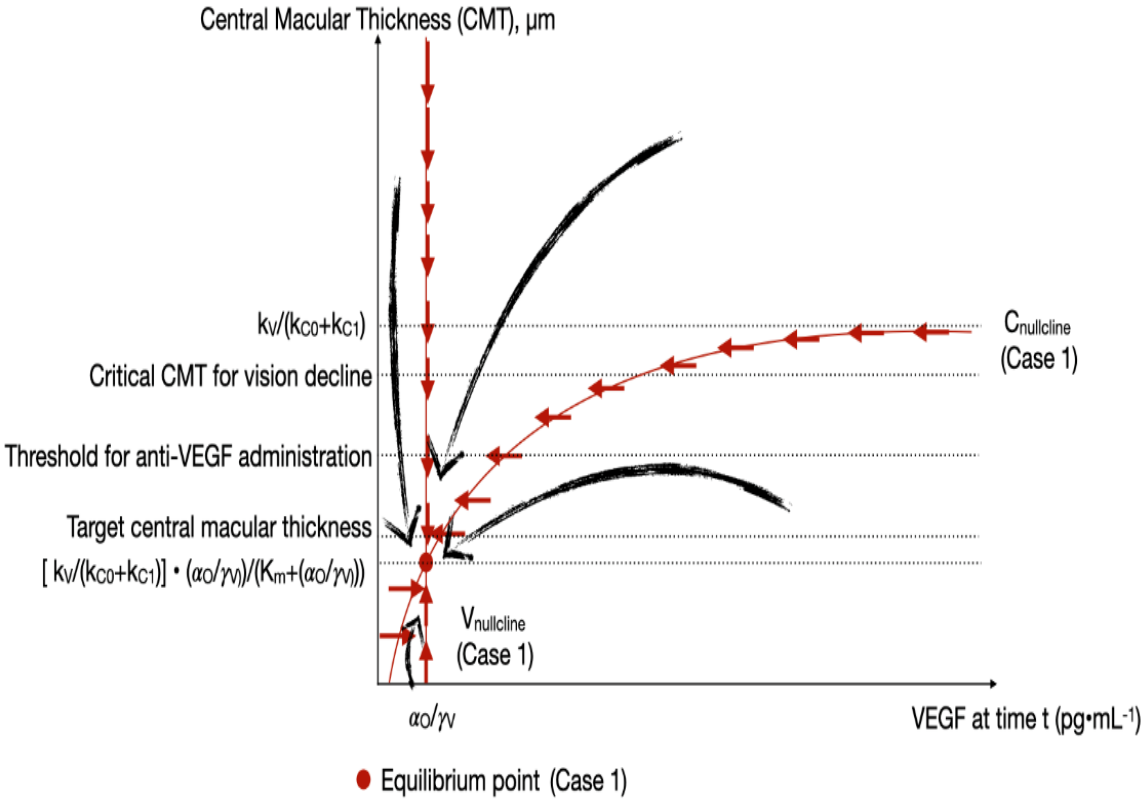

A.4.2 Case 2. Uncontrolled HbA1c, BP or Glycemic Variability. No treatment ($I(t) = 0$) [Figure A2]

This scenario explores the system's behavior when key systemic parameters—specifically HbA1c, BP or glycemic variability —are elevated and uncontrolled, in the absence of anti-VEGF treatment.

A.4.2.1 $V_{nullcline}$ shifts right. With increased HbA1c, BP, and/or glycemic variability (represented by ΔH, ΔB and ΔG respectively), the pathological VEGF production terms become active. $V_{nullcline}$ ($\frac{dV(t)}{dt} = 0$) shifts to the right, meaning a higher steady-state VEGF concentration is required to maintain equilibrium.

From equation (1):

$$\frac{dV(t)}{dt} = \alpha_0 + \alpha_H \cdot \max(0, H(t) - H_0)^n + \alpha_B \cdot \max(0, B(t) - B_0)$$

$$+\alpha_G \cdot \max(0, G(t) - G_0) - \gamma_v \cdot V(t) - \delta_v \cdot I(t) \cdot \frac{V(t)}{K_m + V(t)}$$

When H, B or G are elevated beyond their thresholds (H_0, B_0, G_0), then at least one of the max $(0, \ldots\ldots)$ terms will be positive, contributing to increased VEGF production.

Total VEGF production, termed as P_{VEGF}:

$$P_{VEGF}(H(t), B(t), G(t) = \alpha_0 + \alpha_H \cdot \max(0, H(t) - H_0)^n + \alpha_B \cdot \max(0, B(t) - B_0) + \alpha_G \cdot \max(0, G(t) - G_0)$$

Therefore, when $\frac{dV(t)}{dt} = 0$

$$0 = \alpha_0 + \alpha_H \cdot \max(0, H(t) - H_0)^n + \alpha_B \cdot \max(0, B(t) - B_0)$$

$$+\alpha_G \cdot \max(0, G(t) - G_0) - \gamma_v \cdot V(t) - \delta_v \cdot 0 \cdot \frac{V(t)}{K_m + V(t)}$$

$$= P_{VEGF} - \gamma_v \cdot V(t)$$

Thus:

$$P_{VEGF} = \gamma_v \cdot V(t)$$

$$V(t) = \frac{P_{VEGF}}{\gamma_v}$$

This general form of the $\boldsymbol{V_{nullcline}}$ shows that the steady-state VEGF level is a function of the current (potentially elevated) levels of HbA1c, BP, and glycemic variability, as they contribute to the total VEGF production, P_{VEGF}. When these systemic parameters are uncontrolled and elevated, P_{VEGF} will be higher, leading to the higher steady-state VEGF concentration compared to the controlled scenario.

A.4.2.2 $\boldsymbol{C_{nullcline}}$ shifts up

With increased HbA1c, BP, and/or glycemic variability (represented by ΔH, ΔB and ΔG respectively), the pathological VEGF production terms become active. $\boldsymbol{C_{nullcline}}$ ($\frac{dC(t)}{dt} = 0$) shifts up, meaning for any given VEGF level, the steady-state central macular thickness will be higher than it would be under controlled conditions.

From equation (2):

$$\frac{dC(t)}{dt} = k_v \cdot \frac{V(t-\tau)}{K_m + V(t-\tau)} + \sigma_G \cdot \max(0, G(t) - G_0) \cdot V(t)$$

$$-[k_{c0} + \frac{k_{c1}}{1 + \beta \cdot \max(0, B(t) - B_0)} + \delta_c \cdot I(t)] \cdot C(t)$$

Since the delay τ is small, and the system is in steady state, $V(t-\tau) \approx V(t)$

$$0 = k_v \cdot \frac{V(t)}{K_m + V(t)} + \sigma_G \cdot \Delta G \cdot V(t)$$

$$-[k_{c0} + \frac{k_{c1}}{1 + \beta \cdot \Delta B} + \delta_c \cdot 0] \cdot C(t)$$

$$= k_v \cdot \frac{V(t)}{K_m + V(t)} + \sigma_G \cdot \Delta G \cdot V(t) - [k_{c0} + \frac{k_{c1}}{1 + \beta \cdot \Delta B}] \cdot C(t)$$

Thus:

$$[k_{c0} + \frac{k_{c1}}{1 + \beta \cdot \Delta B}] \cdot C(t) = k_v \cdot \frac{V(t)}{K_m + V(t)} + \sigma_G \cdot \Delta G \cdot V(t)$$

$$C(t) = \frac{1}{k_{c0} + \frac{k_{c1}}{1+\beta \cdot \Delta B}} \cdot [k_v \cdot \frac{V(t)}{K_m + V(t)} + \sigma_G \cdot \Delta G \cdot V(t)]$$

This equation represents $\boldsymbol{C_{nullcline}}$ when HbA1c, BP or glycemic variability are uncontrolled and elevated. In this general case, the terms involving $\max(0, B(t) - B_0)$ and $\max(0, G(t) - G_0)$ remain active in the equation, reflecting their current (elevated) values and their influence on the steady-state central macular thickness.

A.4.2.3 Phase Plane Portrait

2.4.2.3.1 Equilibrium point

When $V(t) = \frac{P_{VEGF}}{\gamma_v}$:

$$\frac{dC(t)}{dt} = k_v \cdot \frac{\frac{P_{VEGF}}{\gamma_v}}{K_m + \frac{P_{VEGF}}{\gamma_v}} + \sigma_G \cdot \Delta G \cdot \frac{P_{VEGF}}{\gamma_v} - [k_{c0} + \frac{k_{c1}}{1+\beta \cdot \Delta B}] \cdot C(t)$$

When $\frac{dC(t)}{dt} = 0$:

$$0 = k_v \cdot \frac{\frac{P_{VEGF}}{\gamma_v}}{K_m + \frac{P_{VEGF}}{\gamma_v}} + \sigma_G \cdot \Delta G \cdot \frac{P_{VEGF}}{\gamma_v} - [k_{c0} + \frac{k_{c1}}{1+\beta \cdot \Delta B}] \cdot C(t)$$

$$[k_{c0} + \frac{k_{c1}}{1+\beta \cdot \Delta B}] \cdot C(t) = k_v \cdot \frac{\frac{P_{VEGF}}{\gamma_v}}{K_m + \frac{P_{VEGF}}{\gamma_v}} + \sigma_G \cdot \Delta G \cdot \frac{P_{VEGF}}{\gamma_v}$$

$$C(t) = \frac{1}{k_{c0} + \frac{k_{c1}}{1+\beta \cdot \Delta B}} \cdot [k_v \cdot \frac{\frac{P_{VEGF}}{\gamma_v}}{K_m + \frac{P_{VEGF}}{\gamma_v}} + \sigma_G \cdot \Delta G \cdot \frac{P_{VEGF}}{\gamma_v}]$$

Thus, the new equilibrium point is

$$(\frac{P_{VEGF}}{\gamma_v}, \frac{1}{k_{c0} + \frac{k_{c1}}{1+\beta \cdot \Delta B}} \cdot [k_v \cdot \frac{\frac{P_{VEGF}}{\gamma_v}}{K_m + \frac{P_{VEGF}}{\gamma_v}} + \sigma_G \cdot \Delta G \cdot \frac{P_{VEGF}}{\gamma_v}])$$

A.4.2.3.2 Vectors along the $V_{nullcline}$:

When $\frac{dC(t)}{dt} > 0$:

$$k_v \cdot \frac{\frac{P_{VEGF}}{\gamma_v}}{K_m + \frac{P_{VEGF}}{\gamma_v}} + \sigma_G \cdot \Delta G \cdot \frac{P_{VEGF}}{\gamma_v} - \left[k_{c0} + \frac{k_{c1}}{1 + \beta \cdot \Delta B}\right] \cdot C(t) > 0$$

$$C(t) < \frac{1}{k_{c0} + \frac{k_{c1}}{1 + \beta \cdot \Delta B}} \cdot [k_v \cdot \frac{\frac{P_{VEGF}}{\gamma_v}}{K_m + \frac{P_{VEGF}}{\gamma_v}} + \sigma_G \cdot \Delta G \cdot \frac{P_{VEGF}}{\gamma_v}]$$

(vectors point upward)

Conversely, when $\frac{dC(t)}{dt} < 0$:

$$C(t) > \frac{1}{k_{c0} + \frac{k_{c1}}{1 + \beta \cdot \Delta B}} \cdot [k_v \cdot \frac{\frac{P_{VEGF}}{\gamma_v}}{K_m + \frac{P_{VEGF}}{\gamma_v}} + \sigma_G \cdot \Delta G \cdot \frac{P_{VEGF}}{\gamma_v}]$$

(vectors point downward)

A.4.2.3.3 Vectors along the $C_{nullcline}$:

From section A.4.2.1, when $\frac{dV(t)}{dt} = 0$:

$$V(t) = \frac{P_{VEGF}}{\gamma_v}$$

When $\frac{dV(t)}{dt} > 0$:

$$V(t) < \frac{P_{VEGF}}{\gamma_v}$$ (vectors point rightward)

Conversely, when $\frac{dV(t)}{dt} < 0$:

$$V(t) > \frac{P_{VEGF}}{\gamma_v}$$ (vectors point leftward)

A.4.2.3.4 Stability of the equilibrium point

From the phase plane portrait, the new equilibrium point is a **sink (stable).**

Figure A2. Phase plane analysis of central macular thickness(CMT) dynamics in Case 2.

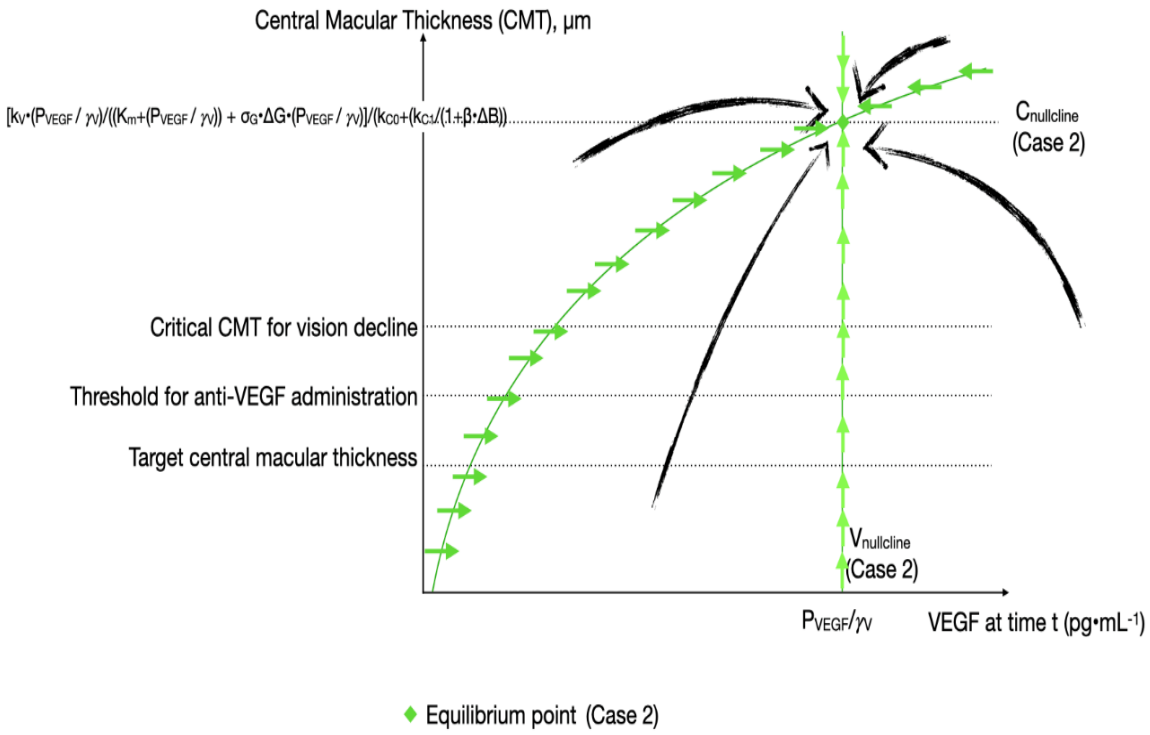

A.4.3 Case 3. Uncontrolled HbA1c ,BP or Glycemic Variability with anti-VEGF treatment ($I(t) = 1$) [Figure A3]

This scenario explores the system's behavior with anti-VEGF treatment when key systemic parameters—specifically HbA1c, BP or glycemic variability —are elevated and uncontrolled.

A.4.3.1 $V_{nullcline}$ shifts left.

From equation (1):

$$\frac{dV(t)}{dt} = \alpha_0 + \alpha_H \cdot \max(0, H(t) - H_0)^n + \alpha_B \cdot \max(0, B(t) - B_0)$$

$$+\alpha_G \cdot \max(0, G(t) - G_0) - \gamma_v \cdot V(t) - \delta_v \cdot I(t) \cdot \frac{V(t)}{K_m + V(t)}$$

Total VEGF production, termed as P_{VEGF}:

$$P_{VEGF}(H(t), B(t), G(t) = \alpha_0 + \alpha_H \cdot \max(0, H(t) - H_0)^n + \alpha_B \cdot \max(0, B(t) - B_0) + \alpha_G \cdot \max(0, G(t) - G_0)$$

Therefore, when $\frac{dV(t)}{dt} = 0$:

$$0 = P_{VEGF} - \gamma_v \cdot V(t) - \delta_v \cdot \frac{V(t)}{K_m + V(t)}$$

Thus:

$$P_{VEGF} = \gamma_v \cdot V(t) + \delta_v \cdot \frac{V(t)}{K_m + V(t)}$$

$$P_{VEGF} = V(t) \cdot \left[\gamma_v + \frac{\delta_v}{K_m + V(t)}\right]$$

$$P_{VEGF} = V(t) \cdot \left[\frac{\gamma_v K_m + \gamma_v V(t) + \delta_v}{K_m + V(t)}\right]$$

Multiply both sides by $K_m + V(t)$:

$$P_{VEGF} \cdot [K_m + V(t)] = V(t) \cdot [\gamma_v K_m + \gamma_v V(t) + \delta_v]$$

$$P_{VEGF} K_m + P_{VEGF} V(t) = \gamma_v K_m V(t) + \gamma_v V(t)^2 + \delta_v V(t)$$

Rearrange into a quadratic equation in terms of $V(t)$:

$$\gamma_v V(t)^2 - (P_{VEGF} - \gamma_v K_m - \delta_v) \cdot V(t) - P_{VEGF} K_m = 0$$

This is a quadratic equation of the form $ax^2 + bx + c = 0$, where:

$$x = V(t),$$
$$a = \gamma_v,$$
$$b = -(P_{VEGF} - \gamma_v K_m - \delta_v),$$
$$c = -P_{VEGF} K_m$$

The VEGF nullcline, $V_{nullcline}$ is given by the positive real solution of the quadratic equation using the quadratic formula:

$$V_{nullcline} = \frac{-\boldsymbol{b}+\sqrt{\boldsymbol{b^2-4ac}}}{\boldsymbol{2a}}$$
$$= \frac{(P_{VEGF} - \gamma_v K_m - \delta_v) + \sqrt{(P_{VEGF} - \gamma_v K_m - \delta_v)^2 + 4\gamma_v P_{VEGF} K_m}}{2\gamma_v}$$

The nullcline represents a new equilibrium with a complex interplay between basal production (α_0), natural VEGF decay (γ_v), and anti-VEGF mediated removal (K_m and δ_v). The saturable nature of VEGF removal implies that while anti-VEGF can significantly reduce VEGF at lower concentrations, there's a limit to how much VEGF it can clear, even if VEGF levels continue to rise. This means that if basal production (α_0) is very high, VEGF may still reach a significant steady state despite treatment.
The presence of the square root and the Michaelis-Menten term (implicitly in the derivation leading to the quadratic formula) means that the steady-state VEGF level is not a simple linear function of its influencing parameters. The interaction between natural decay and saturable anti-VEGF removal creates a more complex, non-linear equilibrium.

A.4.3.2 $C_{nullcline}$ shifts down

From equation (2):

$$\frac{dC(t)}{dt} = k_v \cdot \frac{V(t-\tau)}{K_m + V(t-\tau)} + \sigma_G \cdot \max(0, G(t) - G_0) \cdot V(t)$$

$$-[k_{c0} + \frac{k_{c1}}{1 + \beta \cdot \max(0, B(t) - B_0)} + \delta_c \cdot I(t)] \cdot C(t)$$

Since the delay τ is small, and the system is in steady state, $V(t-\tau) \approx V(t)$:

$$0 = k_v \cdot \frac{V(t)}{K_m + V(t)} + \sigma_G \cdot \Delta G \cdot V(t) - [k_{c0} + \frac{k_{c1}}{1 + \beta \cdot \Delta B} + \delta_c \cdot 1] \cdot C(t)$$

$$= k_v \cdot \frac{V(t)}{K_m + V(t)} + \sigma_G \cdot \Delta G \cdot V(t) - [k_{c0} + \frac{k_{c1}}{1 + \beta \cdot \Delta B} + \delta_c] \cdot C(t)$$

Thus:

$$[k_{c0} + \frac{k_{c1}}{1 + \beta \cdot \Delta B} + \delta_c] \cdot C(t) = k_v \cdot \frac{V(t)}{K_m + V(t)} + \sigma_G \cdot \Delta G \cdot V(t)$$

$$C(t) = \frac{1}{k_{c0} + \frac{k_{c1}}{1 + \beta \cdot \Delta B} + \delta_c} \cdot [k_v \cdot \frac{V(t)}{K_m + V(t)} + \sigma_G \cdot \Delta G \cdot V(t)]$$

This equation represents the effect of anti-VEGF on the $C_{nullcline}$ when HbA1c, BP or glycemic variability are uncontrolled and elevated. In this general case, the terms involving $\max(0, B(t) - B_0)$ and $\max(0, G(t) - G_0)$ remain active in the equation, reflecting their current (elevated) values and their influence on the steady-state central macular thickness.

A.4.3.3 Phase Plane Portrait

A.4.3.3.1 Equilibrium point

Let

$$V_{nullcline} = F = \frac{(P_{VEGF} - \gamma_v K_m - \delta_v) + \sqrt{(P_{VEGF} - \gamma_v K_m - \delta_v)^2 + 4\gamma_v P_{VEGF} K_m}}{2\gamma_v}$$

$$\frac{dC(t)}{dt} = k_v \cdot \frac{V(t)}{K_m + V(t)} + \sigma_G \cdot \Delta G \cdot V(t) - [k_{c0} + \frac{k_{c1}}{1 + \beta \cdot \Delta B} + \delta_c] \cdot C(t)$$

$$= k_v \cdot \frac{F}{K_m + F} + \sigma_G \cdot \Delta G \cdot F - [k_{c0} + \frac{k_{c1}}{1 + \beta \cdot \Delta B} + \delta_c] \cdot C(t)$$

When $\frac{dC(t)}{dt} = 0$:

$$C(t) = \frac{1}{k_{c0} + \frac{k_{c1}}{1+\beta \cdot \Delta B} + \delta_c} \cdot [k_v \cdot \frac{F}{K_m + F} + \sigma_G \cdot \Delta G \cdot F]$$

A.4.3.3.2 Vectors along the $V_{nullcline}$

When $\frac{dC(t)}{dt} > 0$:

$$k_v \cdot \frac{F}{K_m + F} + \sigma_G \cdot \Delta G \cdot F - \left[k_{c0} + \frac{k_{c1}}{1+\beta \cdot \Delta B} + \delta_c\right] \cdot C(t) > 0$$

Thus

$$C(t) < \frac{1}{k_{c0} + \frac{k_{c1}}{1 + \beta \cdot \Delta B} + \delta_c} \cdot [k_v \cdot \frac{F}{K_m + F} + \sigma_G \cdot \Delta G \cdot F]$$

(vectors point upward).

Conversely, when $\frac{dC(t)}{dt} < 0$:

$$C(t) > \frac{1}{k_{c0} + \frac{k_{c1}}{1 + \beta \cdot \Delta B} + \delta_c} \cdot [k_v \cdot \frac{F}{K_m + F} + \sigma_G \cdot \Delta G \cdot F]$$

(vectors point downward).

A.4.3.3.3 Vectors along the $C_{nullcline}$

From section A.4.3.1, when $\frac{dV(t)}{dt} = 0$:

$$P_{VEGF} - \gamma_v \cdot V(t) - \delta_v \cdot \frac{V(t)}{K_m + V(t)} = 0$$

when $\frac{dV(t)}{dt} > 0$:

$$P_{VEGF} - \gamma_v \cdot V(t) - \delta_v \cdot \frac{V(t)}{K_m + V(t)} > 0$$

Rearrange into a quadratic equation in terms of $V(t)$:

$\gamma_v V(t)^2 - (P_{VEGF} - \gamma_v K_m - \delta_v) \cdot V(t) - P_{VEGF} K_m < 0$

The roots are:

$\frac{(P_{VEGF} - \gamma_v K_m - \delta_v) - \sqrt{(P_{VEGF} - \gamma_v K_m - \delta_v)^2 + 4\gamma_v P_{VEGF} K_m}}{2\gamma_v}$ and

$$\frac{(P_{VEGF} - \gamma_v K_m - \delta_v) + \sqrt{(P_{VEGF} - \gamma_v K_m - \delta_v)^2 + 4\gamma_v P_{VEGF} K_m}}{2\gamma_v}$$

Therefore $\frac{dV(t)}{dt} > 0$,

when $\gamma_v V(t)^2 - (P_{VEGF} - \gamma_v K_m - \delta_v) \cdot V(t) - P_{VEGF} K_m < 0$,

when

$$0 < V < \frac{(P_{VEGF} - \gamma_v K_m - \delta_v) + \sqrt{(P_{VEGF} - \gamma_v K_m - \delta_v)^2 + 4\gamma_v P_{VEGF} K_m}}{2\gamma_v}$$

(vectors point rightward)

Conversely $\frac{dV(t)}{dt} < 0$,

when $\gamma_v V(t)^2 - (P_{VEGF} - \gamma_v K_m - \delta_v) \cdot V(t) - P_{VEGF} K_m > 0$,

when $V > \frac{(P_{VEGF} - \gamma_v K_m - \delta_v) + \sqrt{(P_{VEGF} - \gamma_v K_m - \delta_v)^2 + 4\gamma_v P_{VEGF} K_m}}{2\gamma_v}$

(vectors point leftward).

Figure A3. Phase plane analysis of central macular thickness(CMT) dynamics in Case 3.

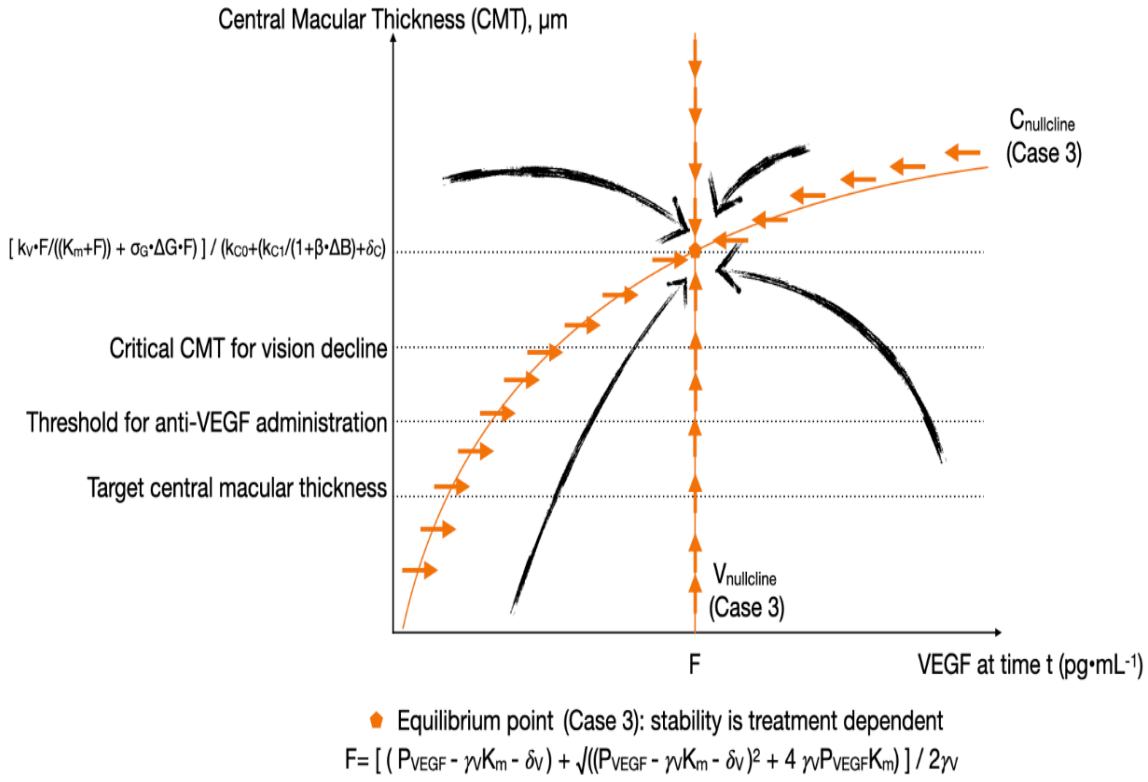

A.4.3.3.4 Stability of the equilibrium point

From the phase plane portrait, the new equilibrium point is a **sink (stable).** However, the observed stability is **fundamentally treatment-dependent**. The system's equilibrium is not globally stable; it is **conditionally stable**, entirely reliant on the presence of active anti-VEGF. This becomes critically apparent when the anti-VEGF wears off and its effect diminishes. At this point, the mathematical nature of the equilibrium changes dramatically: the sink disappears.

Once the anti-VEGF effect wanes, the system's behavior reverts to that of Case 2, which describes an uncontrolled state without treatment. The trajectory, previously drawn towards the temporary sink, now drifts away from the stable point, inevitably towards a pathological attractor if one exists in the absence of intervention. This mirrors the real-world pharmacodynamics of anti-VEGF therapies. Their VEGF-suppressing effect is saturable and temporary (27-42 days for ranibizumab, 3-8 weeks for brolucizumab, 6-8 weeks for aflibercept) [62,63].

Without re-injection, VEGF levels rebound, and macular edema recurs, providing the biological rationale for chronic monthly or treat-and-extend dosing regimens. The equilibrium established in case 3 is thus not a permanent solution but rather a dynamic balance maintained by continuous treatment, highlighting the mechanism behind relapse and the need for ongoing therapy in the DME management.

A.4.4 Model-Derived Equilibrium States: Implications for DME management [Figure A4]

Figure A4 shows the relative positions of equilibrium points in case 1, case 2, and case 3. It visually emphasized the healthier equilibrium achieved with systemic control (Case 1) compared to the pathological equilibrium or attractor of uncontrolled systemic parameters (Case 2). This figure powerfully illustrates how anti-VEGF treatment (Case 3) forces the system into a more desirable, albeit conditionally stable equilibrium, which is distinct from the underlying pathological state of case 2.

This figure distinctly underscores the pivotal role of systemic management in DME. This observed beneficial effect, specifically the reduction or absence of pathological VEGF production, directly results from the effective control of systemic factors such as HbA1c, BP, and glycemic variability. While the intravitreal anti-VEGF therapy, as illustrated in Case 3, effectively manages the downstream consequences of uncontrolled systemic conditions, its efficacy is continuously challenged by ongoing pathological VEGF production if these underlying systemic issues persist. By mitigating this excessive VEGF drive through robust systemic management, the model implicitly demonstrates a multifaceted improvement. This approach can reduce the burden of anti-VEGF therapy, potentially allowing for extended treatment intervals and fewer injections. Furthermore, by addressing the root cause of vascular dysfunction, it can mitigate overall disease progression, aligning with the established long-term benefits seen in landmark studies like UKPDS and DCCT. Consequently, this leads to a significant reduction in treatment and financial burdens for both patients and healthcare systems. This crucial interplay between targeted local anti-VEGF intervention and comprehensive systemic control is fundamental to achieving optimal, sustainable outcomes in DME management.

Figure A4. Comparison of central macular thickness (CMT) dynamics in Case 1, Case 2, and Case 3 within the phase plane.

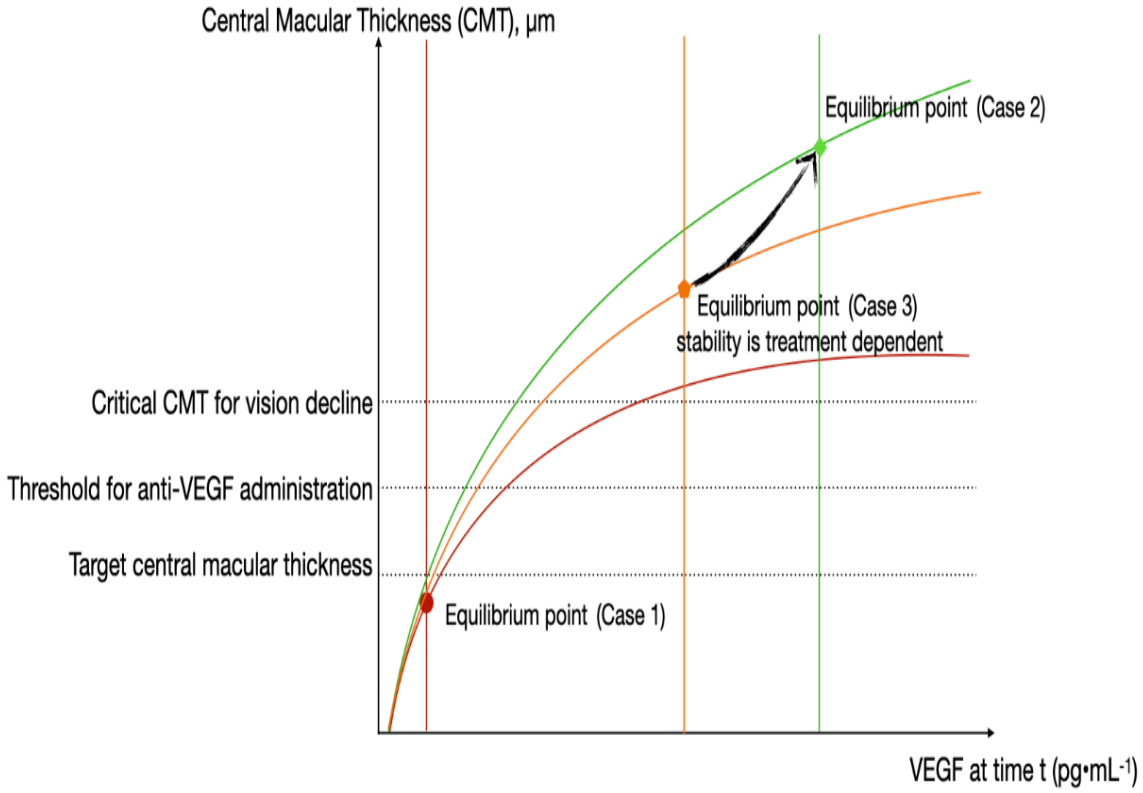

A.4.5 Temporal Dynamics of Central Macular Thickness and Clinical Thresholds [Figure A5]

Figure A5 provides a qualitative illustration of the proposed model's hypothesized impact of metabolic control on central macular thickness dynamics over time. Patients are receiving regular intravitreal anti-VEGF treatment. This conceptual representation aims to highlight the differential long-term outcomes under two distinct scenarios: good metabolic control versus poor metabolic control. The figure's vertical axis denoted central macular thickness in μm, while the horizontal axis represents time in months, overlaid with clinically relevant thresholds for target central macular thickness, anti-VEGF administration, and critical central macular thickness for vision decline.

Figure A5. Hypothesized impact of metabolic control on central macular thickness dynamics over time.

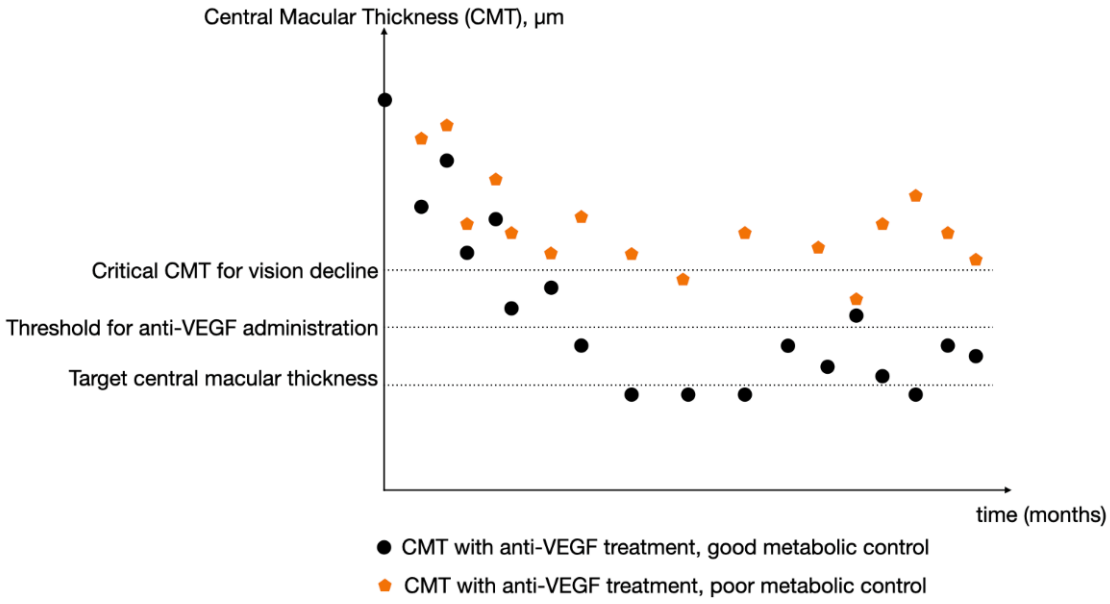

In the scenario depicting good metabolic control (represented by black circles), the model qualitatively predicts a favorable long-term central macular thickness response. Following the initiation of anti-VEGF treatment, central macular thickness is shown to decrease effectively, eventually settling at a steady-state level that consistently remains below the threshold for anti-VEGF administration and often approaches the desired target central macular thickness. This suggests that when underlying systemic drivers of DME are well-managed, anti-VEGF therapy can achieve and sustain optimal anatomical outcomes, reflecting a more receptive ocular environment and reduced pathological VEGF drive.

Conversely, the scenario illustrating poor metabolic control (represented by orange stars) demonstrates a less favorable central macular thickness trajectory, even with ongoing anti-VEGF treatment. While initial treatment may induce some reduction in central macular thickness, the long-term steady-state central macular thickness is hypothesized to remain persistently elevated. In this state, central macular thickness may hover consistently above the threshold for anti-VEGF administration and, at times, even near or above the critical central macular thickness for vision decline. This qualitative difference underscores the model's prediction that unmitigated systemic factors continue to contribute to retinal vascular dysfunction and VEGF production, thereby limiting the full potential of anti-VEGF therapy.

The direct comparison within figure A5 profoundly illustrates the model's central tenet: **systemic metabolic control is an indispensable determinant of long-term anatomical outcomes in DME, even in the context of advanced anti-VEGF therapy**. The distinct steady-state central macular thickness levels achieved under good versus poor metabolic control, despite uniform anti-VEGF intervention suggest that the efficacy of local treatment is significantly modulated by the systemic environment. This implies that controlling factors such as HbA1c, BP and glycemic variability can substantially reduce the residual pathological burden on the ocular system.

From a clinical perspective, these qualitative predictions suggest that achieving and maintaining robust systemic metabolic control could translate into several significant benefits. Patients with well-controlled systemic parameters may require less intensive anti-VEGF regimens (e.g. longer treat-and-extend intervals), potentially leading to fewer injections, better sustained visual acuity, and ultimately, a reduced treatment and financial burden for both individuals and healthcare systems. It is important to note that this figure represents a **conceptual prediction based on the proposed model's qualitative analysis** and serves to highlight hypothesized relationships for further quantitative investigation and empirical validation.

References

1. Kavaric N, Klisic A, Ninic A. Cardiovascular risk estimated by UKPDS risk engine algorithm in diabetes. Open Med (Wars). 2018;13:610-7. doi:10.1515/med-2018-0086
2. Coppens M, Eikelboom JW, Hart RG, et al. The CHA2DS2-VASc score identifies those patients with atrial fibrillation and a CHADS2 score of 1 who are unlikely to benefit from oral anticoagulant therapy. Eur Heart J. 2013;34:170-6. doi:10.1093/eurheartj/ehs314
3. Sharma S, Joshi SN, Karki P. HbA1c as a predictor for response of bevacizumab in diabetic macular oedema. BMJ Open Ophthalmol. 2020;5:e000449. doi:10.1136/bmjophth-2020-000449
4. Dagher C, Akiki M, Saliby R, Harb G. The impact of glycemic control on ranibizumab efficacy in diabetic retinopathy: a retrospective analysis. Cureus. 2025;17:e77124. doi:10.7759/cureus.77124
5. Wong WM, Chee C, Bhargava M, et al. Systemic factors associated with treatment response in diabetic macular edema. J Ophthalmol. 2020;2020:1875860. doi:10.1155/2020/1875860
6. Matsuda S, Tam T, Singh RP, et al. The impact of metabolic parameters on clinical response to VEGF inhibitors for diabetic macular edema. J Diabetes Complications. 2014;28:166-70. doi:10.1016/j.jdiacomp.2013.11.009
7. Boye KS, Thieu VT, Lage MJ, et al. The association between sustained HbA1c control and long-term complications among individuals with type 2 diabetes: a retrospective study. Adv Ther. 2022;39:2208-21. doi:10.1007/s12325-022-02106-4
8. Khalid M, Petroianu G, Adem A. Advanced glycation end products and diabetes mellitus: mechanisms and perspectives. Biomolecules. 2022;12:542. doi:10.3390/biom12040542
9. Tornatore L, Thotakura AK, Bennett J, et al. The nuclear factor kappa B signaling pathway: integrating metabolism with inflammation. Trends Cell Biol. 2012;22:557-66. doi:10.1016/j.tcb.2012.08.001
10. Schmidt AM, Yan SD, Wautier JL, Stern D. Activation of receptor for advanced glycation end products: a mechanism for chronic vascular dysfunction in diabetic vasculopathy and atherosclerosis. Circ Res. 1999;84:489-97. doi:10.1161/01.res.84.5.489
11. Choudhuri S, Chowdhury IH, Das S, et al. Role of NF-κB activation and VEGF gene polymorphisms in VEGF up regulation in non-proliferative and proliferative diabetic retinopathy. Mol Cell Biochem. 2015;405:265-79. doi:10.1007/s11010-015-2417-z
12. Zhang M, Wu J, Wang Y, et al. Associations between blood pressure levels and diabetic retinopathy in patients with diabetes mellitus: a population-based study. Heliyon. 2023;9:e16830. doi:10.1016/j.heliyon.2023.e16830

13. Stana D, Potop V, Istrate SL, et al. Variability of diabetic macular edema in correlation with hypertension retinopathy in patients with diabetes mellitus and essential hypertension. Rom J Ophthalmol. 2019;63:327-38.
14. Lopes de Faria JM, Jalkh AE, Trempe CL, McMeel JW. Diabetic macular edema: risk factors and concomitants. Acta Ophthalmol Scand. 1999;77:170-5. doi:10.1034/j.1600-0420.1999.770211.x
15. Tran EM, Gregori NZ, Rachitskaya A, et al. Systemic predictors of diabetic retinopathy and diabetic macular edema in an adult veteran population. Clin Ophthalmol. 2025;19:101-10. doi:10.2147/OPTH.S487047
16. Lin Z, Wang FH, Wen L, et al. Prevalence of and risk factors for diabetic macular edema in a northeastern Chinese population. Int J Ophthalmol. 2022;15:320-6. doi:10.18240/ijo.2022.02.19
17. Kamoi K, Takeda K, Hashimoto K, et al. Identifying risk factors for clinically significant diabetic macula edema in patients with type 2 diabetes mellitus. Curr Diabetes Rev. 2013;9:209-17. doi:10.2174/1573399811309030002
18. Angaramo S, Liu Y, Chen Q, Padovani-Claudio DA. Impact of hypertension severity on risk of diabetic macular edema development. Invest Ophthalmol Vis Sci. 2021;62:1059.
19. Shah AR, Van Horn AN, Verchinina L, et al. Blood pressure is associated with receiving intravitreal anti-vascular endothelial growth factor treatment in patients with diabetes. Ophthalmol Retina. 2019;3:410-6. doi:10.1016/j.oret.2019.01.019
20. Krogsaa B, Lund-Andersen H, Parving HH, Bjaeldager P. The blood-retinal barrier permeability in essential hypertension. Acta Ophthalmol (Copenh). 1983;61:541-4. doi:10.1111/j.1755-3768.1983.tb04343.x
21. Parving HH, Larsen M, Hommel E, Lund-Andersen H. Effect of antihypertensive treatment on blood-retinal barrier permeability to fluorescein in hypertensive type 1 (insulin-dependent) diabetic patients with background retinopathy. Diabetologia. 1989;32:440-4. doi:10.1007/bf00271264
22. Lightman S, Rechthand E, Latker C, et al. Assessment of the permeability of the blood-retinal barrier in hypertensive rats. Hypertension. 1987;10:390-5. doi:10.1161/01.HYP.10.4.390
23. Suzuma I, Hata Y, Clermont A, et al. Cyclic stretch and hypertension induce retinal expression of vascular endothelial growth factor and vascular endothelial growth factor receptor-2: potential mechanisms for exacerbation of diabetic retinopathy by hypertension. Diabetes. 2001;50:444-54. doi:10.2337/diabetes.50.2.444
24. Hsieh YT, Hsieh MC. Fasting plasma glucose variability is an independent risk factor for diabetic retinopathy and diabetic macular oedema in type 2 diabetes: an 8-year prospective cohort study. Clin Exp Ophthalmol. 2020;48:470-6. doi:10.1111/ceo.13728

25. Chatziralli IP. The role of glycemic control and variability in diabetic retinopathy. Diabetes Ther. 2018;9:431-4. doi.org/10.1007/s13300-017-0345-5
26. Dehghani Firouzabadi F, Poopak A, Samimi S, et al. Glycemic profile variability as an independent predictor of diabetic retinopathy in patients with type 2 diabetes: a prospective cohort study. Front Endocrinol (Lausanne). 2024;15:1383345. doi:10.3389/fendo.2024.1383345
27. Chen B, Shen C, Sun B. Current landscape and comprehensive management of glycemic variability in diabetic retinopathy. J Transl Med. 2024;22:700. doi:10.1186/s12967-024-05516-w
28. Busik JV, Mohr S, Grant MB. Hyperglycemia-induced reactive oxygen species toxicity to endothelial cells is dependent on paracrine mediators. Diabetes. 2008;57:1952-65. doi:10.2337/db07-1520
29. Sun J, Xu Y, Sun S, et al. Intermittent high glucose enhances cell proliferation and VEGF expression in retinal endothelial cells: the role of mitochondrial reactive oxygen species. Mol Cell Biochem. 2010;343:27-35. doi:10.1007/s11010-010-0495-5
30. Risso A, Mercuri F, Quagliaro L, et al. Intermittent high glucose enhances apoptosis in human umbilical vein endothelial cells in culture. Am J Physiol Endocrinol Metab. 2001;281:E924-30. doi:10.1152/ajpendo.2001.281.5.e924
31. Zhang ZY, Miao LF, Qian LL, et al. Molecular mechanisms of glucose fluctuations on diabetic complications. Front Endocrinol (Lausanne). 2019;10:640. doi:10.3389/fendo.2019.00640
32. Shi XL, Ren YZ, Wu J. Intermittent high glucose enhances apoptosis in INS-1 cells. Exp Diabetes Res. 2011;2011:754673. doi:10.1155/2011/754673
33. Lingappan K. NF-κB in oxidative stress. Curr Opin Toxicol. 2018;7:81-6. doi:10.1016/j.cotox.2017.11.002
34. Liu X, Yi M, Jin R, et al. Correlation between oxidative stress and NF-κB signaling pathway in the obesity-asthma mice. Mol Biol Rep. 2020;47:3735-44. doi:10.1007/s11033-020-05466-8
35. Bekyarova GY, Vankova DG, Madjova VH, et al. Association between Nfr2, HO-1, NF-kB expression, plasma ADMA, and oxidative stress in metabolic syndrome. Int J Mol Sci. 2023;24:17067. doi:10.3390/ijms242317067
36. Pierini D, Bryan NS. Nitric oxide availability as a marker of oxidative stress. Methods Mol Biol. 2015;1208:63-71. doi:10.1007/978-1-4939-1441-8_5
37. Ritchie RH, Drummond GR, Sobey CG, et al. The opposing roles of NO and oxidative stress in cardiovascular disease. Pharmacol Res. 2017;116:57-69. doi:10.1016/j.phrs.2016.12.017
38. Förstermann U. Nitric oxide and oxidative stress in vascular disease. Pflugers Arch. 2010;459:923-39. doi:10.1007/s00424-010-0808-2

39. Rossino MG, Lulli M, Amato R, et al. Oxidative stress induces a VEGF autocrine loop in the retina: relevance for diabetic retinopathy. Cells. 2020;9:1452. doi:10.3390/cells9061452
40. Schäfer G, Cramer T, Suske G, et al. Oxidative stress regulates vascular endothelial growth factor-A gene transcription through Sp1- and Sp3-dependent activation of two proximal GC-rich promoter elements. J Biol Chem. 2003;278:8190-8. doi:10.1074/jbc.m211999200
41. Jiang Y, Li J, Zhang J, Chen S. Serum VEGF as a predictive marker of glycemic control and diabetic nephropathy in Chinese older adults with type 2 diabetes mellitus. Front Endocrinol (Lausanne). 2023;14:1274025. doi:10.3389/fendo.2023.1274025
42. Yousif Hussin Alimam H, Abdelateif Hussein W, Ibrahim S, et al. Blood glucose, HbA1c level, and its correlation with VEGF-A (+405g/c) polymorphism as biomarker predicts the risk of retinopathy and nephropathy in type 2 diabetic patients. Rep Biochem Mol Biol. 2022;11:421-9. doi:10.52547/rbmb.11.3.421
43. Zehetner C, Kirchmair R, Kralinger M, Kieselbach G. Correlation of vascular endothelial growth factor plasma levels and glycemic control in patients with diabetic retinopathy. Acta Ophthalmol. 2013;91:e470-3. doi:10.1111/aos.12081
44. Cattoni DI, Chara O, Kaufman SB, et al. Cooperativity in binding processes: new insights from phenomenological modeling. PLoS One. 2015;10:e0146043. doi:10.1371/journal.pone.0146043
45. Baharivand N, Zarghami N, Panahi F, et al. Relationship between vitreous and serum vascular endothelial growth factor levels, control of diabetes and microalbuminuria in proliferative diabetic retinopathy. Clin Ophthalmol. 2012;6:185-91. doi:10.2147/opth.s27423
46. García-Quintanilla L, Luaces-Rodríguez A, Gil-Martínez M, et al. Pharmacokinetics of intravitreal anti-VEGF drugs in age-related macular degeneration. Pharmaceutics. 2019;11:365. doi:10.3390/pharmaceutics11080365
47. Wu Q, Finley SD. Mathematical model predicts effective strategies to inhibit VEGF-eNOS signaling. J Clin Med. 2020;9:1255. doi:10.3390/jcm9051255
48. Owen LA, Hartnett ME. Soluble mediators of diabetic macular edema: the diagnostic role of aqueous VEGF and cytokine levels in diabetic macular edema. Curr Diab Rep. 2013;13:476-80. doi:10.1007/s11892-013-0382-z
49. Shibuya M. Vascular endothelial growth factor (VEGF) and its receptor (VEGFr) signaling in angiogenesis: a crucial target for anti- and pro-angiogenic therapies. Genes Cancer. 2011;2:1097-105. doi:10.1177/1947601911423031
50. Holmes K, Roberts OL, Thomas AM, Cross MJ. Vascular endothelial growth factor receptor-2: structure, function, intracellular signalling and therapeutic inhibition. Cell Signal. 2007;19:2003-12. doi:10.1016/j.cellsig.2007.05.013

51. Sirois MG, Edelman ER. VEGF effect on vascular permeability is mediated by synthesis of platelet-activating factor. Am J Physiol. 1997;272:H2746-56. doi:10.1152/ajpheart.1997.272.6.h2746
52. Mathews MK, Merges C, McLeod DS, Lutty GA. Vascular endothelial growth factor and vascular permeability changes in human diabetic retinopathy. Invest Ophthalmol Vis Sci. 1997;38:2729-41.
53. Bates DO. Vascular endothelial growth factors and vascular permeability. Cardiovasc Res. 2010;87:262-71. doi:10.1093/cvr/cvq105
54. Zhang J, Zhang J, Zhang C, et al. Diabetic macular edema: current understanding, molecular mechanisms and therapeutic implications. Cells. 2022;11:3362. doi:10.3390/cells11213362
55. Sakini ASA, Hamid AK, Alkhuzaie ZA, et al. Diabetic macular edema (DME): dissecting pathogenesis, prognostication, diagnostic modalities along with current and futuristic therapeutic insights. Int J Retina Vitreous. 2024;10:83. doi:10.1186/s40942-024-00603-y
56. Aldokhail LS, Alhadlaq AM, Alaradi LM, et al. Outcomes of anti-VEGF therapy in eyes with diabetic macular edema, vein occlusion-related macular edema, and neovascular age-related macular degeneration: a systematic review. Clin Ophthalmol. 2024;18:3837-51. doi:10.2147/opth.s489114
57. Cheema AA, Cheema HR. Diabetic macular edema management: a review of anti-vascular endothelial growth factor (VEGF) therapies. Cureus. 2024;16:e52676. doi:10.7759/cureus.52676
58. Marmor MF. Mechanisms of fluid accumulation in retinal edema. Doc Ophthalmol. 1999;97:239-49. doi:10.1023/a:1002192829817
59. Hirsch IB. Glycemic variability and diabetes complications: does it matter? Of course it does!. Diabetes Care. 2015;38:1610-4. doi:10.2337/dc14-2898
60. Aiello LP, Bursell SE, Clermont A, et al. Vascular endothelial growth factor-induced retinal permeability is mediated by protein kinase C in vivo and suppressed by an orally effective beta-isoform-selective inhibitor. Diabetes. 1997;46:1473-80. doi:10.2337/diab.46.9.1473
61. Funatsu H, Yamashita H, Shimizu E, et al. Relationship between vascular endothelial growth factor and interleukin-6 in diabetic retinopathy. Retina. 2001;21:469-77. doi:10.1097/00006982-200110000-00009
62. Muether PS, Droege KM, Fauser S. Vascular endothelial growth factor suppression times in patients with diabetic macular oedema treated with ranibizumab. Br J Ophthalmol. 2014;98:179-81. doi:10.1136/bjophthalmol-2013-303954
63. Obata S, Kakinoki M, Sawada O, et al. Duration of vascular endothelial growth factor suppression after intravitreal injection of brolucizumab and aflibercept in macaque eyes. J Ocul Pharmacol Ther. 2023;39:225-8. doi:10.1089/jop.2022.0160